Small regulatory RNAs in vascular remodeling and atherosclerosis

Ingen, E. van

Chapter 5

C/D box snoRNA SNORD113-6 guides 2´O-methylation and protects against site-specific fragmentation of tRNA^{Leu}(TAA) in human arterial fibroblasts

Eva van Ingen[1,2], Pleun A.M. Engbers[1,2], M. Leontien van der Bent[1,2], Hailiang Mei[3], Johann Wojta[4,6], Paul. H.A. Quax[1,2], A. Yaël Nossent[1,2,4-5]

Under review by Molecular Therapy Nucleic Acids

[1]Department of Surgery, [2]Einthoven Laboratory for Experimental Vascular Medicine and [3]Department of Biomedical Data Sciences, Leiden University Medical Center, The Netherlands. [4]Department of Internal Medicine II and [5]Department of Laboratory Medicine, Medical University of Vienna, Austria. [6]Ludwig Boltzmann Institute for Cardiovascular Research, Vienna, Austria.

Abstract

C/D box small nucleolar RNAs (snoRNAs) of the DLK1-DIO3 locus are associated with vascular remodelling and cardiovascular disease. None of these snoRNAs has any known targets yet, except for one, AF357425 in mice and SNORD113-6 in humans. We previously showed that this snoRNA targets mRNAs of the integrin signalling pathway and affects arterial fibroblast function. Here, we aimed to identify whether AF357425/SNORD113-6 can also target small RNAs. We overexpressed or inhibited AF357425 in murine fibroblasts and performed small RNA sequencing. Expression of tRNA fragments (tRFs) was predominantly regulated. Compared to overexpression, AF357425 knockdown led to an overall decrease in tRFs, but with an enrichment in smaller tRFs (<30 nucleotides). We focused on tRNA Leucine anti-codon TAA ($tRNA^{Leu}$(TAA)), that has a conserved predicted binding site for AF357425/SNORD113-6. Adjacent to this site, the tRNA is cleaved to form $tRF^{Leu\ 47\text{-}64}$, in both primary murine fibroblasts and human arterial fibroblasts. We show that AF357425/SNORD113-6 methylates $tRNA^{Leu}$(TAA) and thereby prevents the formation of $tRF^{Leu\ 47\text{-}64}$. Exposing fibroblasts to oxidative or hypoxic stress, increased AF357425/SNORD113-6 and $tRNA^{Leu}$(TAA) expression, but AF357425/SNORD113-6 knockdown did not increase $tRF^{Leu\ 47\text{-}64}$ formation under stress even further. Thus, independent of cellular stress, AF357425/SNORD113-6 protects against site-specific fragmentation of $tRNA^{Leu}$(TAA) via 2'O-ribose-methylation.

Introduction

Small nucleolar RNAs (snoRNAs) are a type of small noncoding RNA that mediate RNA modifications at post-transcriptional level. There are two types of snoRNAs, C/D box and H/ACA box snoRNAs, named after their conserved sequence motifs. C/D box snoRNAs guide 2'-O-ribose methylation (2'Ome) of their target RNAs, whereas H/ACA snoRNAs guide RNA pseudouridylation (Ψ). Both 2'Ome and Ψ are abundant site-specific RNA modifications and are mostly present on ribosomal (r)RNAs, where they function in rRNA folding and translational devotion[1-3].

C/D box snoRNAs associate with four conserved ribonucleoproteins NHP2L1, NOP56, NOP58 and Fibrillarin (FBL). FBL is the methyltransferase that catalyses 2'Ome. C/D box snoRNAs have two antisense boxes, located directly upstream of the D and D' boxes, which are not covered by ribonucleoproteins and are thus free to interact with target RNA sequences. C/D box snoRNAs hybridize to their target RNAs via Watson-Crick base-pairing. Once bound to the target RNA, the 5th nucleotide upstream of the D or D' box is positioned for 2'Ome[1, 2, 4]. Many expressed C/D box snoRNAs, however, lack antisense elements of known rRNA 2'Ome sites and are considered orphan snoRNAs[5]. Likely, these orphan C/D box snoRNAs target other types of RNA molecules than rRNA[6-8].

Besides rRNAs, transfer (t)RNAs are the most heavily modified cellular RNAs[9]. Their canonical function lies in protein translation, where they deliver amino acids to the translating peptide chain. However, recent reports show that tRNAs can be processed into tRNA-derived fragments (tRFs), which can perform other, noncanonical, functions. tRFs can derive from different regions of their parental tRNA, located anywhere from the 5' to 3' end, and have variable sizes up to ~50 nucleotides[10, 11]. Fragmentation of tRNAs can be induced under cellular stress, such as oxidative stress and hypoxia, which are important triggers of vascular remodelling processes[12-14]. Among others, Angiogenin (ANG) is a tRNA-processing endonuclease that is activated during cellular stress[12].

Recent findings show that RNA modifications guided by snoRNAs, 2'Ome and Ψ, can prevent tRNA cleavage and thereby regulate tRF formation[10, 15-18]. For instance, the former orphan SNORD97 induces 2'Ome on the wobble cytidine C34 of tRNA^{Met}(CAT), which protects against ANG-induced cleavage[15]. Loss of pseudouridine synthase 7 (PUS7), a pseudouridylation enzyme guided by H/ACA snoRNAs, results in loss of 5´tRFs of ~18 nucleotides in length, while the production of the larger 5´-tRNA halves increases[16].

The DLK1-DIO3 locus on the long arm of human chromosome 14, encodes a cluster of 41 C/D box snoRNAs (14q32; 12F1 in mice). We have demonstrated that this cluster of 14q32 C/D box snoRNAs is strongly associated with vascular remodelling and human cardiovascular disease[19-21]. The association with cardiovascular disease is both independent of and stronger than the 14q32 long noncoding RNAs (lncRNAs) and the cluster of 14q32 microRNAs that lie adjacent to the snoRNA genes[19]. Furthermore, plasma levels of 14q32 snoRNAs were associated with disease outcome in peripheral arterial disease (PAD) patients[20, 21]. However, all 14q32 C/D box snoRNAs are orphan snoRNAs and their molecular function is still unknown, except for one snoRNA. We recently demonstrated that one of the most abundantly expressed snoRNAs of the 14q32 cluster, human SNORD113-6 and its murine equivalent, AF357425, targets mRNAs of the integrin signalling pathway, influencing both pre-mRNA processing and 2'Ome. The D' antisense box of AF357425/SNORD113-6 is fully conserved between humans and mice. Fibroblast integrin signalling is important for cell-cell and cell-matrix interactions, but also acts in various forms of cardiovascular remodelling that can lead to cardiovascular disease[22]. Indeed, knockdown of SNORD113-6 altered human arterial fibroblast function[23]. Whether AF357425/SNORD113-6 also guides 2'Ome on small RNA molecules, however, is still unknown.

Here, we aimed to determine whether AF357425/SNORD113-6 can target small RNAs. We performed small RNA sequencing (sRNA-seq) on primary murine fibroblasts (PMFs) in which we either inhibited or overexpressed AF357425. We found that tRFs were the predominant group of small RNAs that changed in expression. Knockdown of AF357425 resulted in an apparent reduction of total tRFs, but an enrichment of smaller sized tRFs (18-30 nucleotides). We focused on one of these tRNAs, tRNA Leucine anti-codon TAA ($tRNA^{Leu}$(TAA)), which has a predicted binding site for AF357425 in mice and SNORD113-6 in human. sRNA-seq data showed that its dominant tRF, $tRF^{Leu\ 47\text{-}64}$, is formed just upstream of this site. Formation of $tRF^{Leu\ 47\text{-}64}$ was conserved in both PMFs and human umbilical arterial fibroblasts (HUAFs), and was investigated under oxidative, hypoxic and starvation stress. We show that AF357425/SNORD113-6 indeed methylates this tRNA and protects against site-specific $tRNA^{Leu}$(TAA) fragmentation.

Results

sRNA-seq in primary murine fibroblasts

In order to identify small RNA targets of AF357425/SNORD113-6, we performed sRNA-seq on PMFs in which we either inhibited or overexpressed AF357425. With this strategy, we aimed to obtain the largest possible difference in small RNA target expression. Gapmers were used to inhibit AF357425 expression (GM-AF25) and 3rd Generation Antisense (3GAs) to overexpress AF357425 (3GA-AF25). We showed previously that 3GAs directed against the 3'-end of AF357425 (3GA-AF25) induced snoRNA overexpression, likely through protection from degradation by endonucleases[19]. Expression of AF357425 was increased (>5-fold) in PMFs treated with 3GA-AF, compared to GM-AF25 (Supplemental Figure 1). By far most reads from the sRNA-seq in both samples were mapped to microRNAs. Read counts mapped to microRNAs, as well as those that mapped to the much lower expressed snoRNA and rRNA genes, were similar between AF25-High and AF25-Low cells. However, reads that mapped to tRNA genes, which are all tRFs of <45 nucleotides in length, appeared to be reduced in number in AF25-Low cells (Figure 1A and Supplemental Table 2). Where the longer tRFs (30-45 nucleotides) appeared enriched in AF25-High cells, smaller sized tRFs (18-29 nucleotides) were enriched in AF25-Low cells, particularly the 18-nucleotide tRFs (Figure 1B). These data indicate that AF357425 may direct tRNA fragmentation.

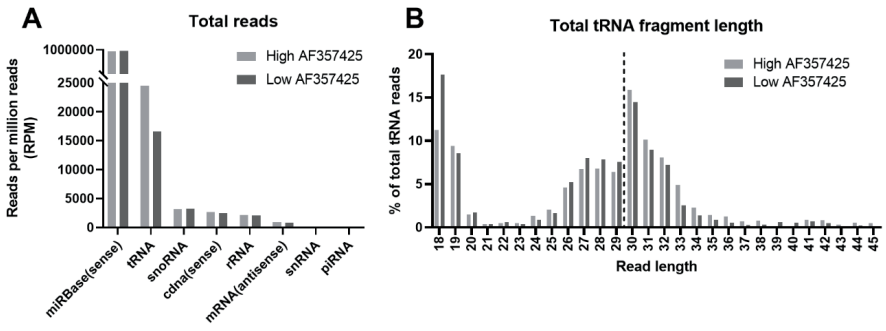

Figure 1. sRNA-seq. (A) Total reads mapped to small RNAs, normalized to reads per million (RPM) and (B) total tRNA fragment length (in nucleotides), shown as a percentage (%) of total tRNA reads in high AF357425 (overexpressed) and low AF357425 (inhibited) primary murine fibroblasts.

Fragmentation of tRNA^{Leu}(TAA)

In order to investigate the mechanisms through which AF357425/SNORD113-6 may influence tRNA fragmentation, we focused on a single tRNA. Among others, tRNA Leucine anti-codon TAA (tRNA^{Leu}(TAA)) had a predicted D' box antisense sequence for AF357425. This site was conserved in human tRNA^{Leu}(TAA) for the D' box antisense sequence of SNORD113-6. Except for the outer 2 nucleotides, a perfect reverse complementary sequence for the middle 7 nucleotides is present in both mouse and human tRNA^{Leu}(TAA) (AACCCCA; Figure 2A). A tRF cleaved just upstream of this predicted 2'Ome site (18 to 20 nucleotides; Figure 2A), tRF$^{Leu\ 47-64}$, was abundantly expressed in both AF25-High and AF25-Low cells (Figure 2B). However, the total tRFs generated from tRNA^{Leu}(TAA) were decreased in AF25-Low cells. In contrast, tRF$^{Leu\ 47-64}$ was more abundant relative to the total tRFs in AF25-Low (50%) compared to AF25-High cells (35%; Figure 2B, C). We confirmed expression of tRF$^{Leu\ 47-64}$ by Northern blot in both PMFs and in HUAFs. Expression of tRF$^{Leu\ 47-64}$ appeared enhanced under oxidative stress (Figure 2D, E).

Validation of tRNA^{Leu}(TAA) 2'Ome

Next, we performed RTL-Q to calculate the EMF, using site-specific primers for detection of 2'Ome. We confirmed 2'Ome of the mature full-length tRNA^{Leu}(TAA), located on the 5th nucleotide upstream of the D' antisense box, in both PMFs and HUAFs. Inhibition of AF357425/SNORD113-6 partly reduced 2'Ome at this site compared to GM-ctrl (p for trend=0.0725 in PMFs and 0.0968 in HUAFs; Figure 3). 2'Ome also appeared present on the precursor-(pre)tRNA^{Leu}(TAA) in HUAFs, but we could not confirm snoRNA-induced regulation of 2'Ome in the pre-tRNA^{Leu}(TAA), due to high Ct values above the detection threshold (>45 Ct; Supplemental Figure 2). The validation of 2'Ome in both mouse and human cells suggests that both are evolutionarily conserved features of tRNA^{Leu}(TAA).

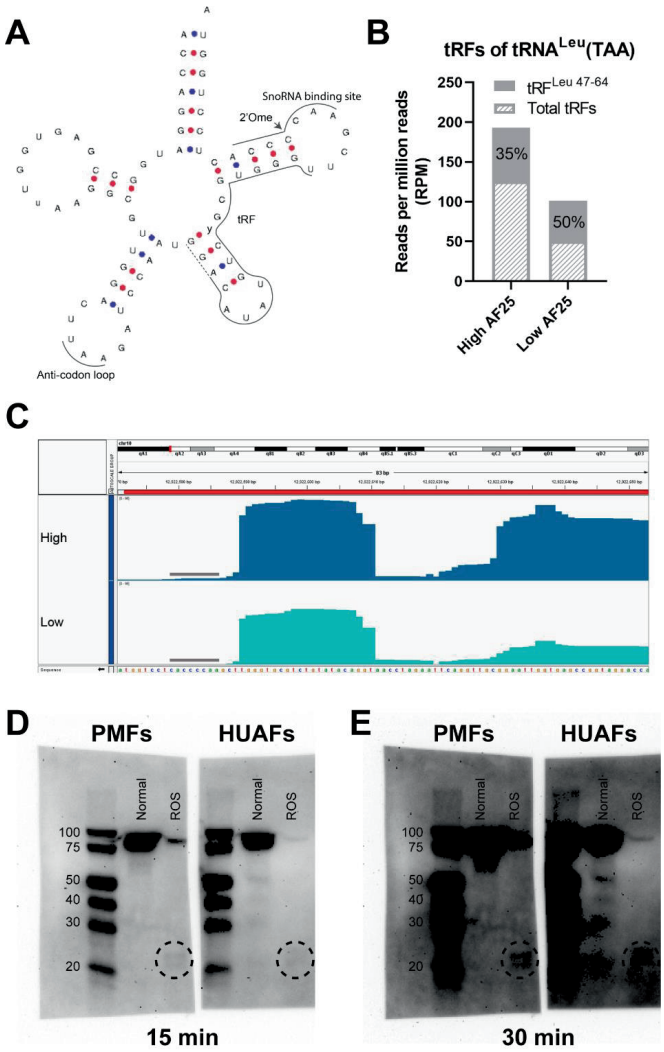

Figure 2. Fragmentation of tRNA^{Leu}(TAA). (A) Schematic overview of the mature tRNA^{Leu}(TAA) sequence in mouse and human. The AF357425/SNORD113-6 predicted binding site (snoRNA binding site), tRNA fragment generated upstream of the binding site, tRF$^{Leu\ 47\text{-}64}$, and the anti-codon loop are indicated with a line. The dashed line indicates length extension of tRF$^{Leu\ 47\text{-}64}$, representing 3 different sizes of generated tRFs. Arrow points at the predicted 2'O-methylation (2'Ome) site. γ represents U in mice and C in human. Figure adapted from GtRNAdb[35]. (B) The fragment of interest, tRF$^{Leu\ 47\text{-}64}$, shown as a percentage of total tRFs generated from tRNA^{Leu}(TAA). Data is normalized to reads per million reads (RPM). (C) Coverage plot of tRNA^{Leu}(TAA) in primary murine fibroblasts with either high or low AF357425 expression. The predicted AF357425 binding site is indicated with a line. Sequence is shown from 3' to 5'. Northern blots exposed for (D) 15 and (E) 30 min using the ChemiDoc-IT imaging system. Primary murine fibroblasts (PMFs) and human umbilical arterial fibroblasts (HUAFs) were cultured in normoxic and oxidative stress (ROS) conditions. A digoxigenin labeled probe was used to visualize tRFs. A circle indicates tRF$^{Leu\ 47\text{-}64}$.

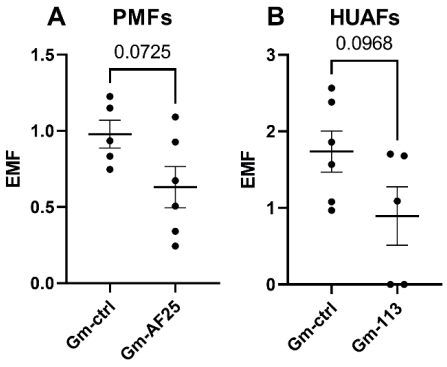

Figure 3. 2'O-methylation at predicted AF357425/SNORD113-6 binding sites on tRNA^{Leu}(TAA). For detection of 2'O-methyated nucleotides and to calculate the estimated methylated fraction (EMF), Reversed Transcription at Low dNTP concentration followed by Quantitative PCR (RTL-Q) was performed. Site-specific reversed primers were used exactly on and 1 nucleotide downstream of the predicted 2'Ome site to accurately determine the exact location of the 2'Ome site. (A) Primary murine fibroblasts (PMFs) or (B) human umbilical arterial fibroblasts (HUAFs) were transfected with Gapmers against AF357425 (GM-AF25)/ SNORD113-6 (GM-113) or a gapmer control (GM-ctrl) for 24 hours. N is represented by the individual dots. Data are represented as mean ±SEM. A two-tailed unpaired t-test was performed to compare GM-AF25/113 with GM-ctrl.

Fragmentation of tRNA^{Leu}(TAA) under cellular stress

As fragmentation of tRNAs can be induced during cellular stress[12-14], we cultured PMFs and HUAFs under different cellular stress conditions and measured expression levels of AF357425/SNORD113-6, mature tRNA^{Leu}(TAA) and tRF$^{Leu\ 47-64}$, by qPCR. Endogenous expression of AF357425/SNORD113-6 and mature tRNA^{Leu}(TAA) showed similar expression patterns in PMFs and HUAFs, with increased expression under both hypoxia and oxidative stress, compared to the normal culture condition control. Serum starvation, on the other hand, did not induce changes in either AF357425/SNORD113-6 or tRNA^{Leu}(TAA) expression compared to normal culture conditions. Expression of tRF$^{Leu\ 47-64}$ was only increased significantly under hypoxia in both PMFs and HUAFs, but appeared slightly elevated under oxidative stress as well (Figure 4).

Subsequently, PMFs and HUAFs were transfected with either GM-AF25/113 or a Gapmer control (GM-ctrl), and were cultured under the different cell stress conditions. The absolute Ct value of mature tRNA^{Leu}(TAA) was divided by the Ct value of tRF$^{Leu\ 47-64}$, in order to quantify expression of tRF$^{Leu\ 47-64}$ relative to mature tRNA^{Leu}(TAA), which it was generated from. The ratio was increased under AF357425/ SNORD113-6 inhibition under control conditions in both PMFs and HUAFs (Figure 5). In PMFs, the ratio was also increased under hypoxia and showed a trend towards an increased ratio under serum starvation (Figure 5A). This increased ratio

demonstrates that more $tRF^{Leu\ 47\text{-}64}$ is formed relative to its mature tRNA, when AF357425/SNORD113-6 is inhibited. When we quantified expression of ANG, we did not observe a difference between GM-AF25/113 and GM-ctrl (Supplemental Figure 3). However, ANG did increase under cellular stress, similar to the snoRNA, both in PMFs and HUAFs. We can neither confirm nor exclude that ANG is responsible for cleavage of $tRNA^{Leu}$(TAA), but we can conclude that ANG is not influenced by the snoRNA directly, and that changes in fragmentation are likely caused by changes in snoRNA-guided 2'Ome of the tRNA.

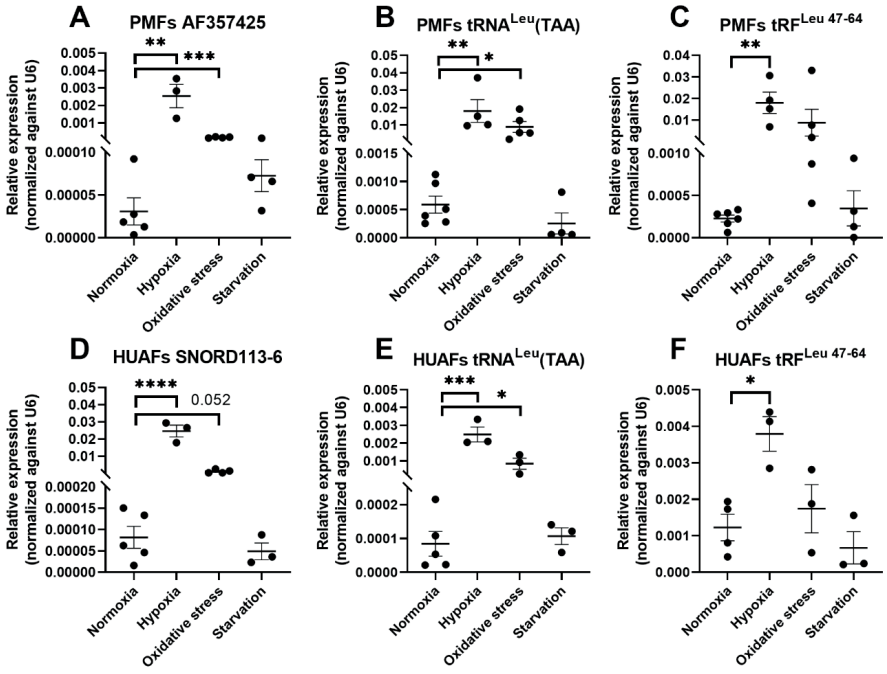

Figure 4. Relative snoRNA, $tRNA^{Leu}$(TAA) and $tRF^{Leu\ 47\text{-}64}$ expression during cellular stress. Relative expression levels in (A-C) primary murine fibroblasts (PMFs) and (D-F) human umbilical arterial fibroblasts (HUAFs) cultured in normoxic, hypoxic, oxidative stress and starvation conditions. Expression levels are normalized to U6. N is represented by the individual dots. Data are represented as mean ±SEM. A two-tailed unpaired t-test was performed to compare treatment with the control. *p<0.05, **p<0.01, ***p<0.005, compared to normoxia.

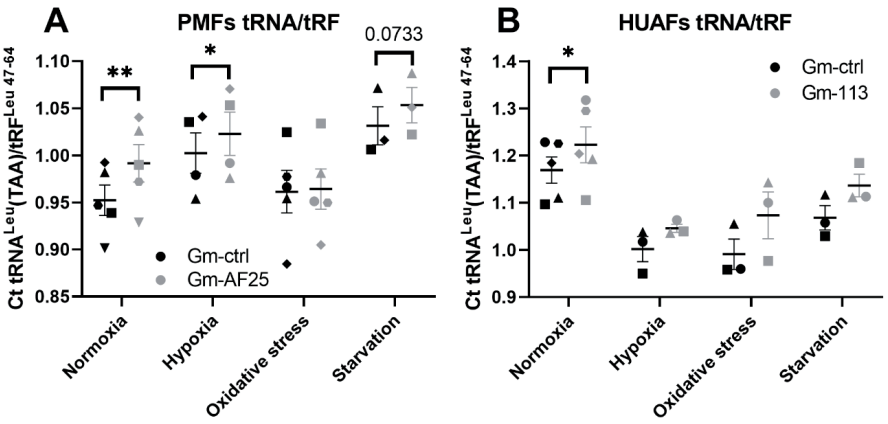

Figure 5. Ratio mature tRNA^{Leu}(TAA)/tRF$^{Leu\ 47\text{-}64}$ in primary cells exposed to different cell stress stimuli. (A) Primary murine fibroblasts (PMFs) and (B) human umbilical arterial fibroblasts (HUAFs) transfected with GM-AF25/113 or GM-ctrl, and cultured in normoxic, hypoxic, oxidative stress or starvation conditions. Expression levels were measured by qPCR. Ratios were calculated by dividing absolute Ct values of the mature tRNA by Ct values of the tRF. N is represented by the individual dots. Data are represented as mean ±SEM. A two-tailed paired t-test was performed to compare single treatment with the control, within each experiment. *p<0.05, **p<0.01, compared to GM-ctrl.

Effects of 2'Ome on tRNA stability

Ribonucleotide modifications in the structural core of the tRNA may stabilize the tRNA and reduce tRNA degradation rates[26]. After transfection with either GM-AF25/113 or GM-ctrl, cells were treated with a high concentration of Actinomycin D (5 µg/µl) for 1h, to inhibit novel tRNA transcription. In both PMFs and HUAFs, mature tRNA^{Leu}(TAA) was rapidly degraded, but no differences were observed between GM-AF25/113 and GM-ctrl (Figure 6A, C). In PMFs, the relative expression of mature tRNA^{Leu}(TAA) was lower to begin with in AF25-Low cells and remained lower after 1h, compared to GM-ctrl (Figure 6A). To rule out differences in degradation rates of housekeeping genes used (RPLP0 and U6) between the two groups, we also normalized the expression levels at 1h to 0h (T0; Figure 6B, D). Indeed, no differences in degradation rates between GM-AF25/113 or GM-ctrl were observed, indicating that a reduction of this single 2'Ome modification did not affect overall mature tRNA^{Leu}(TAA) stability, but only the site-specific fragmentation.

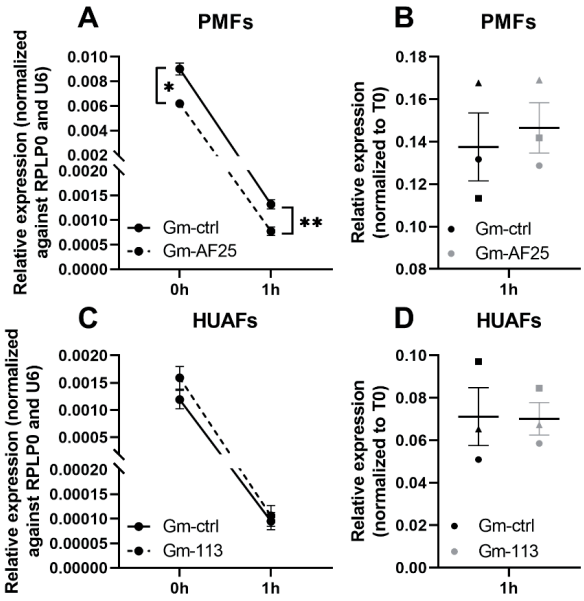

Figure 6. Stability of tRNA^{Leu}(TAA) in primary cells. (A,B) Primary murine fibroblasts (PMFs) and (C,D) human umbilical arterial fibroblasts (HUAFs) were transfected with Gapmers against AF357425 (GM-AF25)/ SNORD113-6 (GM-113) or a gapmer control (GM-ctrl) for 24 hours. After 24 hours, cells were treated for 1 hour with Actinomycin D to inhibit novel RNA transcription. Mature tRNA levels were measured 0 and 1 hour after addition of Actinomycin D. (A,C) Expression levels were normalized to RPLP0 and U6. (B,D) Expression levels at 1h were normalized to 0h (T0). Data are represented as mean ±SEM. *p<0.05, **p<0.01, compared to GM-ctrl.

Discussion

We here aimed to identify small RNA targets of AF357425/SNORD113-6. We found that tRNAs are the predominant small RNA target of AF357425. Inhibition of the snoRNA led to an overall decrease in tRFs, and compared to overexpression of the snoRNA, less larger (>30 nucleotides) and more smaller (<30 nucleotides) tRFs were formed. In order to investigate the underlying mechanisms of action, we focused on tRNA^{Leu}(TAA), which has a conserved binding site for the D' box seed sequence of AF357425/SNORD113-6. We showed that tRNA^{Leu}(TAA) is a 2'Ome target of AF357425/SNORD113-6 and that snoRNA inhibition led to an apparent reduction of 2'Ome at this site, both in murine and in human cells. Endogenous expression of AF357425/SNORD113-6 and mature tRNA^{Leu}(TAA), both increased under hypoxia and oxidative stress. Endogenous tRF$^{Leu\ 47\text{-}64}$ expression was also elevated under hypoxia. Knockdown of AF357425/SNORD113-6 resulted in an increased ratio of tRF$^{Leu\ 47\text{-}64}$ relative to its mature tRNA^{Leu}(TAA), particularly under normal culture conditions, without induction of cellular stress. 2'Ome by AF357425/SNORD113-6 was not important for the overall stability of the tRNA, however, we show that it acts via protecting against site-specific fragmentation of tRNA^{Leu}(TAA).

The same post-transcriptional modifications on tRNAs have been shown to both protect from and promote fragmentation[16, 17]. Our data suggest that AF357425/SNORD113-6 2'Ome protects the tRNA from cleavage into small fragments (~18 nucleotides in length), rather than promoting it. However, we found more tRFs in total, including all tRFs formed of tRNA^{Leu}(TAA), and longer fragments (>30 nucleotides) in AF357425-High cells than in AF357425-Low cells. Perhaps the presence or absence of modifications attracts different tRNA endonucleases, which produce different tRF species. However, the expression of mature tRNAs may also be different between AF357425-High and -Low cells and this could of course also affect total tRF production, e.g. expression of tRNA^{Leu}(TAA) decreased under knockdown of AF357425. The role of AF357425/SNORD113-6 2'Ome in cleavage of other tRNAs remains to be determined, but likely, its function is to prevent fragmentation of shorter tRFs (~18 nucleotides in length), as we demonstrated for tRNA^{Leu}(TAA).

Besides the stabilizing tertiary structure, little is known about other functions of post-transcriptional modifications in the structural core of tRNAs[26]. AF357425/SNORD113-6 targets and guides 2'Ome in the T-arm, the structural core, of tRNA^{Leu}(TAA). 2´Ome and the formation of tRF$^{Leu\ 47\text{-}64}$, were found in mouse and human cells, suggesting that both are evolutionarily conserved features of tRNA^{Leu}(TAA). Degradation rates of tRNA^{Leu}(TAA) were similar between GM-ctrl and GM-AF25/113 transfected cells, indicating that 2'Ome by

AF357425/SNORD113-6 is not important for the overall tRNA^{Leu}(TAA) stability. Of course, tRNAs are heavily modified and reduction of a single 2'Ome modification may not have direct consequences for their stability. Also, as knockdown of AF357425/SNORD113-6 only partly reduced 2'Ome and not completely, this reduction may not have been sufficient for decreasing tRNA stability. Nevertheless, we show that 2'Ome by AF357425/SNORD113-6 at least acts in preventing fragmentation of a specific site within tRNA^{Leu}(TAA).

The lack of effects on overall stability of tRNA^{Leu}(TAA) indicates that the presence of other modifications on the tRNA is similar between GM-ctrl or GM-AF25/113 treated cells, meaning that the single 2'Ome site is likely the only modification placed by AF357425/SNORD113-6 on this particular tRNA. The tRNA does, most likely, carry other modifications. This could pose a threat to the reliability of our measurements. Modifications on tRNAs may impede reverse transcription and limit detection of tRFs and tRNAs by rt/qPCR[27]. However, 2'Ome by AF357425/SNORD113-6 is located towards the 3' end of the tRNA. We designed qPCR primers for mature tRNA^{Leu}(TAA) upstream of that site, in order to limit confounding effects by presence or absence of 2'Ome. Furthermore, expression of tRF$^{Leu\ 47-64}$, that we initially found in the sRNA-seq, was confirmed by Northern blot and our qPCR results showed that tRF$^{Leu\ 47-64}$ and mature tRNA^{Leu}(TAA) were both abundantly expressed. We cannot control for effects of other modifications in our qPCRs, however, if reversed transcription was hampered by other modifications, these were likely similar between GM-AF25/113 and GM-ctrl.

Recent studies have shown that fragmentation of tRNAs increases under cellular stress[12-14, 28]. Similar cellular stress conditions, such as ischemia that leads to hypoxia in the underlying tissues, also trigger vascular remodelling processes. This implicates that the formation of tRFs may even play a role in vascular remodelling. Oxygen-glucose deprivation, which is an *in vitro* model for ischemic reperfusion injury, induced tRNA cleavage in neuronal cells[14]. Also, *in vivo* in ischemic brain tissue and in a hindlimb ischemia model, the formation of tRFs was strongly increased[13]. Similarly, we have previously shown that the 14q32 snoRNAs are regulated under ischemic conditions in PAD patients and during vascular remodeling[19]. In the current study, we show that expression of AF357425/SNORD113-6 indeed increased during hypoxia and oxidative stress, but not during serum starvation. Exposing cells to cellular stress did not result in an additional increase of tRF$^{Leu\ 47-64}$ to mature tRNA^{Leu}(TAA) ratio in AF357425/SNORD113-6 knockdown cells, whereas expression of mature tRNA^{Leu}(TAA) and ANG increased under both hypoxia and oxidative stress. In fact, the strongest increase in tRF$^{Leu\ 47-64}$/mature tRNA^{Leu}(TAA) ratio was observed in cells cultured under physiological conditions. An explanation could be that ANG and other endonucleases are being activated during cellular

stress[12, 28], which generate alternative tRF species from tRNA^{Leu}(TAA). We found no differences between GM-ctrl and GM-AF25/113 in relative ANG expression, and thus AF357425/SNORD113-6 does not directly regulate ANG expression. However, it could also be that the dramatic upregulation of the snoRNA under stress conditions completely overruled that relatively subtle knockdown of the snoRNA that we achieved with Gapmer treatment.
The question remains what the function of this AF357425/SNORD113-6-dependent tRF$^{Leu\ 47-64}$ could be. Assumingly, tRF$^{Leu\ 47-64}$ has an important role in cell physiology, as tRF$^{Leu\ 47-64}$ is also generated under physiological conditions and not exclusively during cellular stress. Our group, as well as others, have shown that tRFs have potential as circulating biomarkers in, for example, acute stroke[29-31]. It has also been demonstrated that tRFs can perform all sorts of regulatory functions, including regulation of protein translation, microRNA-like functions by base-pairing with mRNAs and interaction with RNA-binding proteins[32, 33]. Furthermore, tRFs have been shown to be functionally active in modulating cardiac and skeletal muscle function, endothelial function, but also in inhibition of angiogenesis[13, 34]. Which exact regulatory function(s) this particular tRF may have and how it impacts cellular function remains to be determined.

Taken together, we show that AF357425/SNORD113-6 targets predominantly tRNAs, protecting the tRNA from cleavage into small fragments. When zooming in on one specific tRNA, tRNA^{Leu}(TAA), we show that AF357425/SNORD113-6 induces 2'Ome of the mature tRNA, thereby protecting against site-specific tRNA fragmentation. The function of tRF$^{Leu\ 47-64}$, in general and in vascular remodelling in particular, remains to be elucidated.

Material and methods

Cell culture

Cells were cultured in a humidified incubator at 37°C under 5% CO_2. Cells were passaged at 70-90% confluency and used up to passage 6. DMEM, supplemented with 10% heat-inactivated foetal calf serum (FCSi) and 1% Pen/Strep, was used as culture media and was refreshed every 2-3 days.

Primary murine fibroblasts (PMFs) isolation

Ear tissues from C57BL/6-J mice, about 3 weeks of age, were clipped into smaller pieces and embedded in 0.2% gelatine in 6-well plates. DMEM supplemented with 20% FCSi and 1% non-essential amino acids (NEAA; Thermo Fisher, MA, USA, Cat.Nr.11140050), was added to the embedded ear-clippings. After 7 days, skin fibroblasts were grown out of the tissues onto the bottom of the culture plates. PMFs were expanded in culture media up to passage 3. PMFs were then used for further analysis or frozen down and stored in liquid nitrogen for later use.

Primary human umbilical arterial fibroblasts (HUAFs) isolation

Umbilical cords from full-term pregnancies were collected, stored in sterile PBS at 4°C, and within 7 days used for HUAFs isolation. The two arteries were isolated from the umbilical cord. Endothelial cells were removed by gently rolling the artery over a blunted needle. After that, the tunica adventitia and tunica media were separated using surgical tools. The tunica adventitia was incubated overnight in culture media supplemented with 10% heat inactivated human serum (PAA, Pasching, Austria) and 1% NEAA. The next day, the tunica adventitia was treated with 2 mg/ml collagenase type II solution (Worthington; OH, USA, Cat.Nr.NC9693955) at 37°C. The resulting cell suspension was filtered over a 70 µm cell strainer and centrifuged at 400g for 10 minutes. Cells were plated in 6-wells plates and media was refreshed after 90 minutes to remove slow adhering non-fibroblasts cells. HUAFs were expanded up to passage 3, used for further analysis or frozen down and stored in liquid nitrogen for later use.

Cellular stress conditions

Oxidative stress in both PMFs and HUAFs was induced by adding 10 µM of ROS mimic tert-butyl hydroperoxide (tBHT; Luperox, 458139, Sigma Aldrich, MO, USA) to the culture media for 24h. To serum starve the cells, DMEM with 1% PenStrep, supplemented with 1% FCSi for PMFs or 3% FCSi for HUAFs, was added to the cells for 24h. To induce hypoxia, cells in normal culture media were kept in a humidified incubator at 37°C under 1% O_2 for 24h.

RNA isolation and RT/qPCR

RNA was isolated by standard TRIzol (Thermo Fisher, MA, USA, Cat.Nr.15596026) chloroform extractions. RNA concentration and purity were measured using Nanodrop (Nanodrop Technologies, DE, USA) or the Bioanalyzer (2100 Bioanalyzer Instrument, Agilent, CA, USA). Reversed transcription of total RNA was performed with the high-capacity RNA-to-cDNA reverse transcription kit (Applied Biosystems, Thermo Fisher, MA, USA, Cat.Nr.4388950). Quantitect SybrGreen reagents (Qiagen Benelux, Venlo, the Netherlands, Cat.Nr.204145) were used for quantifications. Custom designed TaqMan small RNA assays (Thermo Fisher, Cat.Nr.4398987) were used for reversed transcription and quantifications of tRFs. Expression levels were normalized to U6 using the $2^{-\Delta Ct}$ method. All primers used are provided in Supplemental Table 1.

3rd Generation Antisense and Gapmers

3rd Generation Antisense oligonucleotides (3GAs) were kindly provided by Idera Pharmaceuticals (Cambridge, MA, USA). 3GAs directed to AF357425, consisted of two identical strands of DNA-nucleotides with a full phosphorothioate backbone, connected by a 5' phosphorothioate linker. Gapmers (GM) were custom designed against AF357425 (GM-AF25) or SNORD113-6 (GM-113; Sigma Aldrich, MO, USA). GM were made up out of five 2'Ome RNA-nucleotides, ten DNA-nucleotides and five more 2'Ome RNA-nucleotides with full phosphorothioate backbone. Sequences of 3GAs and GM are provided in Supplemental Table 1.

Transfection with 3rd Generation Antisense and Gapmers

Prior to transfections, G1 cell cycle arrest was induced by treating cells with KN-93 (Sigma Aldrich, MO, USA, Cat.Nr.K1385), an inhibitor of CaMK-II (the multifunctional Ca2+/CaM kinase). KN-93 was added to the culture media at a concentration of 10 μM for 48h. After cell synchronization, cells were washed with PBS and basal DMEM was added. Meanwhile, lipofectamine RNAiMAX Reagent (ThermoFisher, MA, USA, Cat.Nr.13778030) was used to create micelles loaded with 3GAs (200 nM) or GM (500 nM) against snoRNA AF357425 or SNORD113-6 for transfection. Micelles were added to the cells and after 1h of transfection, 10% FCSi was supplemented to the transfected cells. After 24h of transfection, cells were washed with PBS and used for further experiments or analyses.

RNA sequencing and analysis

RNA was isolated from PMFs transfected with 3GA or GM against AF357425. Isolated RNA was shipped to BGI for DNBseq sRNA-seq (GEO: GSE190537). Generated sRNA-seq files in

FASTQ format are processed using the sRNAbench tool[24]. Bowtie aligner was used to align reads to various reference genome and databases, such as GRCm38, mirbase small database, and RNAcentral. The expression of multiple classes of small RNA are quantified in the single assignment based approach where reads mapping to multiple loci are assigned to the locus that has the highest expression. RPM (Read per million) normalized counts are further generated that are used for downstream analysis.

Northern blotting

Total RNA samples were diluted in Novex Tris-borate-EDTA (TBE)-Urea sample buffer (ThermoFisher, Cat.Nr.LC6876), denatured at 95^{o}C for 5 minutes and put on ice. 15% Mini-PROTEAN TBE-Urea gels (BioRad, Cat.Nr.4566053) in TBE buffer were pre-run at 200 V for 20 minutes. After that, RNA samples and digoxigenin (DIG)-labeled Blue Color Marker for small RNA (DynaMarker, BioDynamics, Cat.Nr.DM270-125uL) were loaded on the gel. Gels were electrophoresed at 200 V for ~1h. Next, RNA was transferred from the gel to a Hybond N+ membrane (GE Healthcare, Cat.Nr.RPN203B) at 200 mA for 1h. A Mini Trans-Blot Electrophoretic Transfer Cell (Biorad) system with an ice element and stirrer were used for RNA transfer. Next, RNA was crosslinked to the membrane with freshly prepared 1-ethyl-3-(3-dimethylaminopropyl) carbodiimide (EDC; Sigma, Cat.Nr.E1769) 1-methylimidazole (Sigma, Cat.Nr.336092) crosslinking solution (pH 8) for 1h at 60^{o}C. Membranes were pre-hybridized in ULTRAhyb Oligo Hybridization Buffer (Invitrogen, Cat.Nr.AM8663) at 37^{o}C for 30 min while gently shaking. Dual DIG-labelled DNA probes (designed and ordered at Integrated DNA Technologies, NJ, USA) were denatured at 95^{o}C for 1 min, added to the hybridization buffer (final concentration 5 nM) and left overnight at 37^{o}C. The next day, membranes were washed with low stringency wash buffer (2x SSC, 0.1% SDS), high stringency was buffer (0.1x SSC, 0.1% SDS) at 37^{o}C and then washed with 2x SSC buffer at room temperature. Then, membranes were washed and blocked with the DIG Wash and Block Buffer Set (Roche, Cat.Nr.11585762001) according to the manufacture's protocol. After blocking for 3h at room temperature while shaking, Anti-Digoxigenin-AP, Fab fragments (Roche, Cat.Nr.11093274910) in blocking buffer (1:15.000) were added to the membranes. CDP-star Development Reagent (Roche, Cat.Nr.CDP-RO) was added to the membranes and images were acquired using ChemiDoc-IT imaging system. Dual DIG-labelled DNA probes are listed in Supplemental Table 1.

Detection of 2'Ome

For detection of 2'Ome nucleotides we used an adaptation of the Reverse Transcription at Low dNTP concentration followed by Quantitative PCR (RTL-Q) method that was described by

Dong et al. To accurately determine the exact location of the 2'Ome site on mature tRNA, a reversed primer downstream of the 2'Ome site (R_D) and a reversed primer on the 2'Ome site (R_U) were designed to the +1 and 0 nt downstream of the predicted 2'Ome nucleotide, respectively. The RT reaction was performed in two consecutive steps. First, a mixture of 20 ng RNA and 10 µM R_D or R_U primers was denatured at 70^{o}C for 5 minutes and incubated at 42^{o}C for 10 minutes as an initial annealing step. Then, a high (200µM) or low (0,5µM) concentration of dNTPs (Promega, Cat.Nr.U1511), 200U of M-MLV reverse transcriptase (Promega, Cat.Nr.M1705) and 20U of Recombinant RNasin Ribonuclease Inhibitor (Promega, Cat.Nr.N2515) was added to the RT reaction. The RT reaction was incubated at 42^{o}C for 90 minutes followed by incubation at 75^{o}C for 15 minutes. When a 2'Ome site is present, the extension of the R_D primer pauses at this site when low dNTP concentrations are used, whereas the R_U primer does not. Primer extensions are not affected by 2'Ome sites when performing RT at high dNTP concentrations. The differences in RT products were quantified by SYBR green-based qPCR. The estimated methylated fraction (EMF) was calculated using the following formula.

EMF = (Ct Low dNTP R_D – Ct High dNTP R_D) – (Ct Low dNTP R_U – Ct High dNTP R_U)
>0 means that methylation is present
≤0 means that no methylation is present

The sequence of the human precursor tRNA (pre-tRNA) was obtained from publicly available RNA sequencing data performed by Gogakos et al[25]. RT primers were designed around the predicted 2'Ome site. One reverse primer was designed upstream of the possible 2'Ome site (R_U) and one downstream of the 2'Ome site (R_D). One forward primer (FW) was used for both R_U and R_D. The same RTL-Q conditions were used as for mature tRNA. All primer sequences are provided in Supplemental Table 1.

Degradation assay

HUAFs and PMFs were treated with KN-93 for 48h and then transfected with GM-113 or GM-AF25, respectively, or a negative GM-ctrl, as described above. After 24h of transfection, cells were treated with 5 µg/µl Actinomycin D (Sigma Aldrich, Cat.Nr.A9415) to inhibit novel RNA transcription for 1h. The decline of mature tRNA and the tRF levels over time were quantified by qPCR.

Statistical analyses

Results are expressed as mean ± standard error of the mean (SEM). An unpaired t-test was performed to compare single treatment with the control. As knockdown efficiency varied per experiment, for these experiments a paired t-test was performed to compare each treatment with its own control, within each individual experiment. Graphpad (v.9.0.1) was used to perform all statistical analysis. $p<0.05$ was considered significant and $p<0.1$ was considered a trend.

Author contributions

E.V.I., P.H.A.Q. and A.Y.N. designed the experiments; E.V.I., P.A.M.E., M.L.B. and H.M. conducted the experiments; E.V.I., J.W., P.H.A.Q. and A.Y.N. wrote, reviewed and edited the paper; A.Y.N. acquired funding; A.Y.N. and P.H.A.Q. supervised.

Conflict of interest

There are no conflicts of interest.

Key words

tRNA fragments; C/D box small nucleolar RNAs; orphan; 14q32 locus; DLK1-DIO3 locus; cardiovascular disease

References

1. Watkins, N.J., and Bohnsack, M.T. (2012). The box C/D and H/ACA snoRNPs: key players in the modification, processing and the dynamic folding of ribosomal RNA. *Wiley Interdiscip Rev RNA* **3**: 397-414.
2. Kiss, T. (2001). Small nucleolar RNA-guided post-transcriptional modification of cellular RNAs. *The EMBO journal* **20**: 3617-3622.
3. Decatur, W.A., and Fournier, M.J. (2002). rRNA modifications and ribosome function. *Trends Biochem Sci* **27**: 344-351.
4. Ojha, S., Malla, S., and Lyons, S.M. (2020). snoRNPs: Functions in Ribosome Biogenesis. *Biomolecules* **10**.
5. Jorjani, H., Kehr, S., Jedlinski, D.J., Gumienny, R., Hertel, J., Stadler, P.F., Zavolan, M., and Gruber, A.R. (2016). An updated human snoRNAome. *Nucleic Acids Res* **44**: 5068-5082.
6. Falaleeva, M., Welden, J.R., Duncan, M.J., and Stamm, S. (2017). C/D-box snoRNAs form methylating and non-methylating ribonucleoprotein complexes: Old dogs show new tricks. *Bioessays* **39**.
7. Elliott, B.A., Ho, H.T., Ranganathan, S.V., Vangaveti, S., Ilkayeva, O., Abou Assi, H., Choi, A.K., Agris, P.F., and Holley, C.L. (2019). Modification of messenger RNA by 2'-O-methylation regulates gene expression in vivo. *Nature communications* **10**: 3401.
8. Nostramo, R.T., and Hopper, A.K. (2019). Beyond rRNA and snRNA: tRNA as a 2'-O-methylation target for nucleolar and Cajal body box C/D RNPs. *Genes & development* **33**: 739-740.
9. Pereira, M., Francisco, S., Varanda, A.S., Santos, M., Santos, M.A.S., and Soares, A.R. (2018). Impact of tRNA Modifications and tRNA-Modifying Enzymes on Proteostasis and Human Disease. *Int J Mol Sci* **19**.
10. Krishna, S., Raghavan, S., DasGupta, R., and Palakodeti, D. (2021). tRNA-derived fragments (tRFs): establishing their turf in post-transcriptional gene regulation. *Cell Mol Life Sci* **78**: 2607-2619.
11. Keam, S.P., and Hutvagner, G. (2015). tRNA-Derived Fragments (tRFs): Emerging New Roles for an Ancient RNA in the Regulation of Gene Expression. *Life (Basel)* **5**: 1638-1651.
12. Fu, H., Feng, J., Liu, Q., Sun, F., Tie, Y., Zhu, J., Xing, R., Sun, Z., and Zheng, X. (2009). Stress induces tRNA cleavage by angiogenin in mammalian cells. *FEBS Lett* **583**: 437-442.
13. Li, Q., Hu, B., Hu, G.W., Chen, C.Y., Niu, X., Liu, J., Zhou, S.M., Zhang, C.Q., Wang, Y., and Deng, Z.F. (2016). tRNA-Derived Small Non-Coding RNAs in Response to Ischemia Inhibit Angiogenesis. *Scientific reports* **6**: 20850.
14. Elkordy, A., Mishima, E., Niizuma, K., Akiyama, Y., Fujimura, M., Tominaga, T., and Abe, T. (2018). Stress-induced tRNA cleavage and tiRNA generation in rat neuronal PC12 cells. *J Neurochem* **146**: 560-569.
15. Vitali, P., and Kiss, T. (2019). Cooperative 2'-O-methylation of the wobble cytidine of human elongator tRNA(Met)(CAT) by a nucleolar and a Cajal body-specific box C/D RNP. *Genes & development* **33**: 741-746.
16. Guzzi, N., Cieśla, M., Ngoc, P.C.T., Lang, S., Arora, S., Dimitriou, M., Pimková, K., Sommarin, M.N.E., Munita, R., Lubas, M., et al. (2018). Pseudouridylation of tRNA-Derived Fragments Steers Translational Control in Stem Cells. *Cell* **173**: 1204-1216.e1226.
17. Lyons, S.M., Fay, M.M., and Ivanov, P. (2018). The role of RNA modifications in the regulation of tRNA cleavage. *FEBS Lett* **592**: 2828-2844.
18. Clouet d'Orval, B., Bortolin, M.L., Gaspin, C., and Bachellerie, J.P. (2001). Box C/D RNA guides for the ribose methylation of archaeal tRNAs. The tRNATrp intron guides the formation of two ribose-methylated nucleosides in the mature tRNATrp. *Nucleic Acids Res* **29**: 4518-4529.
19. Håkansson, K.E.J., Goossens, E.A.C., Trompet, S., van Ingen, E., de Vries, M.R., van der Kwast, R., Ripa, R.S., Kastrup, J., Hohensinner, P.J., Kaun, C., et al. (2019). Genetic associations and regulation of expression indicate an independent role for 14q32 snoRNAs in human cardiovascular disease. *Cardiovascular research* **115**: 1519-1532.

20. Håkansson, K.E.J., Sollie, O., Simons, K.H., Quax, P.H.A., Jensen, J., and Nossent, A.Y. (2018). Circulating Small Non-coding RNAs as Biomarkers for Recovery After Exhaustive or Repetitive Exercise. *Front Physiol* **9**: 1136.
21. Nossent, A.Y., Ektefaie, N., Wojta, J., Eichelberger, B., Kopp, C., Panzer, S., and Gremmel, T. (2019). Plasma Levels of snoRNAs are Associated with Platelet Activation in Patients with Peripheral Artery Disease. *Int J Mol Sci* **20**.
22. Civitarese, R.A., Kapus, A., McCulloch, C.A., and Connelly, K.A. (2017). Role of integrins in mediating cardiac fibroblast-cardiomyocyte cross talk: a dynamic relationship in cardiac biology and pathophysiology. *Basic Res Cardiol* **112**: 6.
23. Ingen, E., Homberg, D.A.L., Bent, M.L., Mei, H., Papac-Milicevic, N., Kremer, V., Boon, R.A., Quax, P.H.A., Wojta, J., and Nossent, A.Y. (2021). C/D box snoRNA SNORD113-6/AF357425 plays a dual role in integrin signalling and arterial fibroblast function via pre-mRNA processing and 2'O-ribose methylation. *Human molecular genetics*.
24. Aparicio-Puerta, E., Lebrón, R., Rueda, A., Gómez-Martín, C., Giannoukakos, S., Jaspez, D., Medina, J.M., Zubkovic, A., Jurak, I., Fromm, B., et al. (2019). sRNAbench and sRNAtoolbox 2019: intuitive fast small RNA profiling and differential expression. *Nucleic Acids Res* **47**: W530-w535.
25. Gogakos, T., Brown, M., Garzia, A., Meyer, C., Hafner, M., and Tuschl, T. (2017). Characterizing Expression and Processing of Precursor and Mature Human tRNAs by Hydro-tRNAseq and PAR-CLIP. *Cell reports* **20**: 1463-1475.
26. Motorin, Y., and Helm, M. (2010). tRNA stabilization by modified nucleotides. *Biochemistry* **49**: 4934-4944.
27. Potapov, V., Fu, X., Dai, N., Corrêa, I.R., Jr., Tanner, N.A., and Ong, J.L. (2018). Base modifications affecting RNA polymerase and reverse transcriptase fidelity. *Nucleic Acids Res* **46**: 5753-5763.
28. Yamasaki, S., Ivanov, P., Hu, G.F., and Anderson, P. (2009). Angiogenin cleaves tRNA and promotes stress-induced translational repression. *J Cell Biol* **185**: 35-42.
29. Nguyen, T.T.M., van der Bent, M.L., Wermer, M.J.H., van den Wijngaard, I.R., van Zwet, E.W., de Groot, B., Quax, P.H.A., Kruyt, N.D., and Nossent, A.Y. (2020). Circulating tRNA Fragments as a Novel Biomarker Class to Distinguish Acute Stroke Subtypes. *Int J Mol Sci* **22**.
30. Ishida, T., Inoue, T., Niizuma, K., Konno, N., Suzuki, C., Inoue, T., Ezura, M., Uenohara, H., Abe, T., and Tominaga, T. (2020). Prediction of Functional Outcome in Patients with Acute Stroke by Measuring tRNA Derivatives. *Cerebrovasc Dis* **49**: 639-646.
31. Magee, R., Londin, E., and Rigoutsos, I. (2019). TRNA-derived fragments as sex-dependent circulating candidate biomarkers for Parkinson's disease. *Parkinsonism Relat Disord* **65**: 203-209.
32. Su, Z., Wilson, B., Kumar, P., and Dutta, A. (2020). Noncanonical Roles of tRNAs: tRNA Fragments and Beyond. *Annu Rev Genet* **54**: 47-69.
33. Magee, R., and Rigoutsos, I. (2020). On the expanding roles of tRNA fragments in modulating cell behavior. *Nucleic Acids Res* **48**: 9433-9448.
34. Liapi, E., van Bilsen, M., Verjans, R., and Schroen, B. (2020). tRNAs and tRNA fragments as modulators of cardiac and skeletal muscle function. *Biochim Biophys Acta Mol Cell Res* **1867**: 118465.
35. . GtRNAdb tRNAscan-SE analysis of complete genomes. June 2021 ed.

Supplementary data

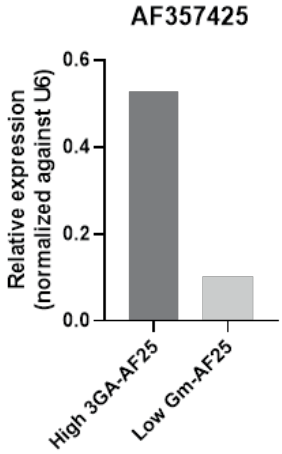

Supplemental Figure 1: Relative AF357425 expression in small RNA-seq samples. Primary murine fibroblasts were transfected with 3rd Generation Antisense (High 3GA-AF25) or Gapmers (Low Gm-AF25) against AF357425 for 24 hours. Expression levels are normalized to U6.

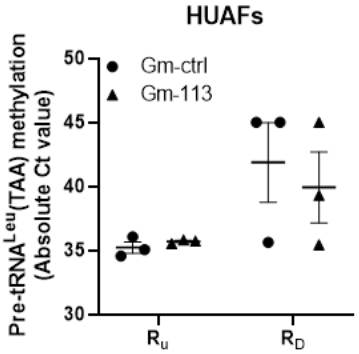

Supplemental Figure 2. Precursor (pre-)tRNA^{Leu}(TAA) methylation in human arterial fibroblasts (HUAFs). For detection of 2'O-methyated nucleotides, Reversed Transcription at Low dNTP concentration followed by Quantitative PCR (RTL-Q) was performed. Reversed primers were designed upstream (R_U) and downstream (R_D) of the predicted 2'O-methylation (2'Ome) site. RT was performed at low dNTP concentrations. When a 2'Ome site is present, the extension of the R_D primer pauses at this site when low dNTP concentrations are used, whereas the R_U primer does not. Results are shown in absolute Ct values. Ct values above the detection threshold are shown as 45 Ct. N is represented by the individual dots.

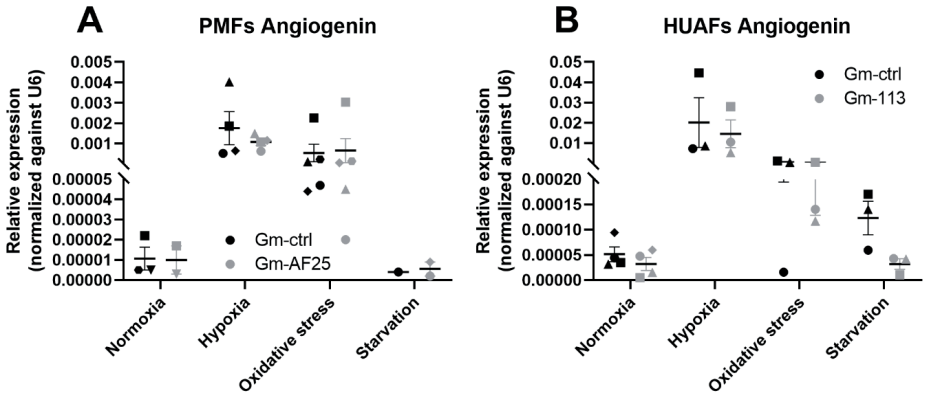

Supplemental Figure 3. Angiogenin expression in primary cells during cellular stress. (A) Primary murine fibroblasts (PMFs) and (B) human umbilical arterial fibroblasts (HUAFs) were transfected with either Gm-ctrl or Gm-AF25/113 and cultured in normoxic (control), hypoxic, oxidative stress or starvation conditions for 24h. Relative expression levels are normalized to U6. N is represented by the individual dots.

Oligonucleotide	
3GA-AF357425	3’-[GGGTTTAATCACTGTCCTC]$_D$-X-[CTCCTGTCACTAATTTGGG]$_D$-3’
GM-AF357425-D’	3’-[GUCAG]$_{2'OmeR}$[AAACCCCATG]$_D$[CUCCU]$_{2'OmeR}$-5’
GM-113-6-D’	3’-[CAGAA]$_{2'OmeR}$[ACCCCATGAT]$_D$[ATTCA]$_{2'OmeR}$-5’
GM-Control	3’-[AUCGA]$_{2'OmeR}$[TACCGTATAA]$_D$[UAACG]$_{2'OmeR}$-5’
Northern blot	
Dual DIG-labelled DNA probes	/5Dig/ACCCACGCAGACATATGT/3Dig/
Methylation primers	
Mature tRNA^{Leu}(TAA) HSA/MMU FW	CCGAGTGGTTAAGGCGTTG
Mature tRNA^{Leu}(TAA) HSA/MMU R$_D$	TGGTACCAGGAGTGG
Mature tRNA^{Leu}(TAA) HSA/MMU R$_U$	GGTACCAGGAGTGGG
pre-tRNA^{Leu}(TAA) HSA FW	AAACAAGGTTCAACGTCTGCA
pre-tRNA^{Leu}(TAA) HSA R$_D$	ACCTAAAGCTACCAGGAGTGG
pre-tRNA^{Leu}(TAA) HSA R$_U$	CGAACCCACGCGGACATATG
qPCR primers	
Mature tRNA^{Leu}(TAA) FW	CCGAGTGGTTAAGGCGTTG
Mature tRNA^{Leu}(TAA) RV	CAGGAGTGGGGTTCGAAC
Taqman Custom designed	
tRF$^{47-64}$ MMU	UGGACAUAUGUCUGCGUGGGU
tRF$^{47-64}$ HSA	UGGACAUAUGUCCGCGUGGGU
Housekeeping genes	
U6– MMU/HSA – FW	AGAAGATTAGCATGGCCCCT
U6– MMU/HSA – RV	ATTTGCGTGTCATCCTTGCG
RPLP0 HSA FW	TCCTCGTGGAAGTGACATCG
RPLP0 HSA RV	TGTCTGCTCCCACAATGAAAC
RPLP0 MMU FW	GTGATGCCCAGGGAAGACAG
RPLP0 MMU RV	TCTGCTCCCACAATGAAGCA
SnoRNAs	
SNORD113-6 – FW	TGGACCAGTGATGAATATCATG
SNORD113-6 – RV	TGGACCTCAGAGTTGCAGATG
AF357425 – FW	AGGAGCATGGGGTTTCTGAC
AF357425 – RV	TTTCATAAGGGTTTAATCACTGTCC
Angiogenin	
HSA FW	CTGGGCGTTTTGTTGTTGGTC
HSA RV	GGTTTGGCATCATAGTGCTGG
MMU FW	CCAGGCCCGTTGTTCTTGAT
MMU RV	GCAAACCATTCTCACAGGCAATA

Supplemental Table 1. Oligonucleotide and primer sequences. 3rd Generation Antisense (3GA) and gapmers (GM). [nnn]$_D$ = DNA-nucleotides; [nnn]$_{2'OmeR}$ = 2’Ome-RNA nucleotides; X = phosphorothioate linker.

antiCodon	High RPM	Low RPM	FoldChange
AlaAGC	342	317	1,08
AlaCGC	169	198	0,85
AlaTGC	334	387	0,86
ArgACG	686	338	2,03
ArgCCG	304	188	1,61
ArgCCT	1000	637	1,57
ArgTCG	786	376	2,09
ArgTCT	235	227	1,04
AsnGTT	446	101	4,40
AspGTC	1109	628	1,77
CysGCA	159	106	1,50
GlnCTG	144	150	0,96
GlnTTG	85	79	1,07
GluCTC	1153	735	1,57
GluTTC	640	489	1,31
GlyACC	22	13	1,67
GlyCCC	167	179	0,94
GlyGCC	817	806	1,01
GlyTCC	322	445	0,72
HisATG	2	2	1,09
HisGTG	213	160	1,33
IleAAT	957	811	1,18
IleGAT	11	7	1,66
IleTAT	20	16	1,20
LeuAAG	256	382	0,67
LeuCAA	255	178	1,43
LeuCAG	272	221	1,23
LeuTAA	238	121	1,97
LeuTAG	157	217	0,72
LysCTT	1758	1357	1,30
LysTTT	1241	1156	1,07
MetCAT	984	437	2,25
PheGAA	250	99	2,53
ProAGG	853	347	2,46
ProCGG	726	355	2,04
ProTGG	2659	1319	2,02
SeC(e)TCA	16	7	2,19
SeCTCA	1	1	0,67
SerAGA	470	406	1,16
SerCGA	77	44	1,75
SerGCT	139	74	1,88
SerGGA	25	8	2,95
SerTGA	161	144	1,12

SupTTA	3	1	2,42
ThrAGT	203	192	1,06
ThrCGT	148	87	1,69
ThrTGT	280	188	1,49
TrpCCA	333	245	1,36
TyrGTA	1610	736	2,19
ValAAC	233	178	1,30
ValCAC	328	261	1,26
ValTAC	88	85	1,04

Supplemental Table 2. Expression of tRNA fragments in reads per million (RPM). Small RNA sequencing was performed on primary murine fibroblasts with AF357425 overexpression (High) and knockdown (Low). Fold change is calculated by dividing High by Low RPM. Read counts are quantified in the single assignment approach where reads that map to multiple loci are assigned to the locus that has the highest expression.